RESEARCH ARTICLE

Continuous Coverage Control of UAVs Based on Cluster Reconfiguration in the Context of Counterattack

XINGLONG GU[ID], GUIFEN CHEN, ZICHEN SUN, AND YIMING SUN
School of Electronic and Information Engineering, Changchun University of Science and Technology, Changchun 130022, China
Corresponding author: Guifen Chen (2020100674@mails.cust.edu.cn)

ABSTRACT UAV clusters are the main application form of multi-intelligence for the intelligent era. Especially in the context of strikes, UAV clusters become an efficient weapon resource on the battlefield by their flexible mobility, no casualties, and low cost. This paper studies the UAV continuous coverage control method based on cluster reconfiguration in the strike context. Firstly, a consistent formation control law for UAVs based on 4-connection topology is proposed based on consistency theory to achieve cluster control and continuous coverage of UAVs. Secondly, a virtual repair trajectory is designed based on the disengaged formation set, and a continuous coverage control law is designed based on the sliding mode theory to solve the topological damage and discontinuous coverage of UAV clusters. Finally, simulation experiments show that the proposed method has obvious performance improvement in UAV cluster reconfiguration convergence time and continuous coverage control, effectively guaranteeing the robustness, destructiveness, and timeliness of UAV cluster reconfiguration.

INDEX TERMS Combat background, UAV clusters, formation reconfiguration, continuous coverage control.

I. INTRODUCTION

UAVs have played a huge advantage in armed reconnaissance strikes, emergency danger rescue, and daily detection and monitoring due to their flexible and safe application, low cost, efficient and stable performance [1], [2], [3]. However, due to the large limitations of energy, load, and performance of UAVs, it is still difficult to perform huge and complex tasks, while UAV clusters can make up for these shortcomings and break through the technical barriers. UAV clustering cannot be separated from the support of various technologies such as formation reconfiguration, mission assignment, trajectory planning, and intelligent decision-making. For example, in the literature [4], a multi-objective optimization method based on an improved genetic algorithm is proposed for the real-time assignment problem of maximizing mission

The associate editor coordinating the review of this manuscript and approving it for publication was Arun Prakash[ID].

value, which effectively solves the cooperative problem of heterogeneous multi-UAV mission planning. In the literature [5], a search-resampling-optimization (SRO) framework was proposed to solve the problem of efficient and robust autonomous scheduling during trajectory planning in complex obstacle scenarios. Similarly, continuous UAV coverage control is also an important technology to support multiple UAVs in complex and difficult missions. Continuous UAV coverage clustering refers to the integration of a certain number of UAVs to form a network-level multi-intelligent body movement system with independent generation and autonomous maintenance, thereby achieving real-time coverage of the reconnaissance area. In the context of enemy strikes, differences in the clustering approach will determine the performance differences that exist in the formations. The literature [6] proposed a distributed control strategy that exploits explicit coordination errors between robots to achieve accurate leader-following formations. The

literature [7] proposed a hierarchical grouped leader-following structure to enable UAVs to achieve global asymptotic stability under control input constraints. In the literature [8], based on the loosely coupled structure, the center of the UAV-BS motion trajectory is regarded as an imaginary point to form a rigid body, as a way to reduce the control difficulty and computational capability requirements of the UAV-BS formation. The literature [9] proposed to map bird flock flight mechanisms to UAV cluster systems, enabling coordinated autonomous control of UAV cluster formation. In [10], a composite vector artificial potential field method was proposed to achieve UAV obstacle avoidance in 3D space in the form of formation. The literature [11] proposed a consistency method with minimum adjustment constraint, which can make the UAV converge to the specified position quickly and realize distributed and fast cluster formation of UAVs. The literature [12] proposed a trajectory planning method based on optimal control and transforms the formation problem into a loose formation constraint to participate in optimization, achieving time-optimal trajectory generation and stable formation. In a striking context, a stable formation structure and efficient maneuverability are the characteristics required for UAV cluster formations, so a distributed, reliable and flexible approach to cluster formation needs to be explored to deal with the ever-changing dynamics of the battlefield.

As the formation will be subject to different degrees of enemy strikes, resulting in the formation's continuity coverage against the reconnaissance area will not be guaranteed and the communication topology will be damaged. The minimally adjusted 3D formation strategy based on consistency theory proposed in the literature [13] can achieve arbitrary switching of formation shapes and reconfigure the cluster network. The literature [14] proposed a consistency algorithm-based UAV cluster formation strategy that enables UAVs to form formations safely and stably while satisfying maneuverability constraints. In the literature [15], it is proposed to abstract the UAV formation problem as a multi-objective optimization problem with soft and hard constraints and design an improved pigeon flock optimization algorithm to obtain the Pareto bound. In the literature [16], a consistent formation method that takes into account the communication delay and interaction topology is proposed to properly solve the problem of formation asymmetric interference and network congestion. The literature [17] proposed an event-triggered time-lag discrete formation controller to effectively reduce the communication load for formation control. A flux-guided path planning method is proposed in the literature [18], which can generate collision-free trajectories for multiple UAVs and maximize the target coverage. The literature [19] proposed an intelligent self-organizing node deployment method based on the idea of molecular equilibrium to move nodes only in the neighborhood to achieve low energy consumption with maximum coverage of the detection area. The literature [20] proposed an improved

self-organizing mapping (SOM) algorithm that takes into account the mobile distance and energy, which can effectively heal the coverage holes, reduce the energy consumption and improve the network lifetime. The literature [21] proposed a hierarchical planning approach for map scanning and task assignment, which leads to comprehensive visual coverage of large-scale outdoor scenes. The highly dynamic, multi-variable battlefield environment in the strike context with the formation characteristics of continuous coverage exacerbates the difficulty of UAV cluster anti-attack technology. Therefore, the UAV cluster continuous coverage control method in the strike context should have the advantages of accurate repair, fast convergence, and lowest energy consumption to improve the life cycle and strike resistance of the formation.

As one of the best representatives of unmanned systems, UAV cluster reconfiguration should be highly robust. The literature [22] abstracted the formation reconfiguration problem as an optimization model considering energy consumption and completion time and solved the desired position for the minimum cost movement of the UAV using a small traversal search. The literature [23] proposed a method to select target expectation points for UAVs using a target location selection algorithm and then transform the reconstruction problem into an expectation point tracking problem. The literature [24] proposed the design of a cooperative controller for UAV cluster reconfiguration by applying the integral sliding mode control theory under the communication topology switching condition, which ensures the robustness and stability of the UAV reconfiguration process. The literature [25] proposed a reconfiguration method combining the UAV formation model and fast expanding random tree to achieve fast reconfiguration of UAV clusters in complex environments. The literature [26] proposed a collaborative decentralized formation reconfiguration framework as a solution to reconfigure the formation in case of UAV failure. The literature [27] proposed an adaptive hybrid particle swarm optimization and differential evolution algorithm for minimizing the total travel distance of UAV reconfiguration, thus reducing the cost of formation reconfiguration. The literature [28] proposed to apply distributed model predictive control to transform the formation recon-figuration problem into an optimization problem and apply a quantum particle swarm algorithm to accelerate the computation as a way to improve the model-solving accuracy and UAV cluster reconfiguration efficiency. However, all the above algorithms need to change the members of the whole formation and fail to effectively use the space resources to achieve fast and accurate reconfiguration of the cluster; therefore, it is important to investigate the reconfiguration strategy of the UAV cluster for the robustness and adaptation of the UAV cluster to intelligent and complex battlefield conditions.

In this paper, we study the continuous coverage control of UAV cluster formation based on consistency theory and sliding mode theory when the communication topology is 4-connected in a striking context. The UAVs realize cluster

formation based on consistency control law, and in the event of enemy strikes, the virtual desired trajectory can be calculated based on the data situation of the disengaged formation set and the tail-end repair UAVs, and the non-singular fast terminal sliding mode method is applied to track the trajectory while maintaining the attitude stability of the UAVs to achieve UAV cluster reconfiguration and complete the repair and topology reconstruction of the reconnaissance hole, avoiding the large-scale movement of the entire formation caused by The problems such as long formation convergence time, difficult control and resource wastage occur.

II. UAV CLUSTER PROBLEM DESCRIPTION AND SYSTEM MODELING

In this chapter, the concepts of the UAV single-engine model, consistency theory, sliding mode theory, and graph theory are introduced, while the problem scenario to be solved is described mathematically to provide the theoretical basis for the subsequent solution.

A. UAV MODEL

The physical quantities in the UAV model can be represented by the Earth's inertial coordinate system or the airframe coordinate system $U(x^u, y^u, z^u)$. The transformation matrix from the airframe coordinate system to the Earth inertial coordinate system can be expressed by performing Euler angular matrix calculations for the yaw angle φ, pitch angle θ and roll angle ψ as [29]:

$$R_{U \to G}$$
$$= \begin{bmatrix} C\psi C\theta & C\psi S\theta S\varphi - S\psi C\varphi & C\psi S\theta C\varphi + S\psi S\varphi \\ S\psi C\theta & S\psi S\theta S\varphi + C\psi C\varphi & S\psi S\theta C\varphi - C\psi S\varphi \\ -S\theta & C\theta S\varphi & C\theta C\varphi \end{bmatrix} \tag{1}$$

Usually, the position physical quantities of UAVs are represented under the earth inertial reference system and the UAV attitude physical quantities are represented under the airframe coordinate system. The UAV flight can be described by the kinetic model and the kinematic model. In this paper, we consider n isomorphic UAV for clustering, and the dynamics equation of the ith UAV can be expressed by the derivation of Lagrange's equation under the condition of considering external disturbance as:

$$\begin{bmatrix} \ddot{x}_i \\ \ddot{y}_i \\ \ddot{z}_i \\ \ddot{\varphi}_i \\ \ddot{\theta}_i \\ \ddot{\psi}_i \end{bmatrix} = \begin{bmatrix} U_{uav}^{li} R_{U \to G}^{(13)} - \Gamma_{i1}^{uav} \dot{x}_i/m + d_{xi}(t) \\ U_{uav}^{li} R_{U \to G}^{(12)} - \Gamma_{i2}^{uav} \dot{x}_i/m + d_{yi}(t) \\ U_{uav}^{li} R_{U \to G}^{(11)} - \Gamma_{i3}^{uav} \dot{x}_i/m - g + d_{zi}(t) \\ U_{uav}^{\varphi i} - d^u \Gamma_{i4}^{uav} \dot{\varphi}_i/I_\varphi + d_{\varphi i}(t) \\ U_{uav}^{\theta i} - d^u \Gamma_{i5}^{uav} \dot{\theta}_i/I_\theta + d_{\theta i}(t) \\ U_{uav}^{\psi i} - d^u \Gamma_{i6}^{uav} \dot{\psi}_i/I_\psi + d_{\psi i}(t) \end{bmatrix} \tag{2}$$

where $(x_i, y_i, z_i)i = 1, \ldots, n$ denotes the position coordinates of the UAV under the earth inertial reference system, $(\varphi_i, \theta_i, \psi_i)$ denotes the attitude angle coordinates of the UAV under the airframe coordinate system,

$(U_{uav}^{li}, U_{uav}^{\varphi i}, U_{uav}^{\theta i}, U_{uav}^{\psi i})$ denotes the control input for the position and attitude of the UAV, Γ_i^{uav} denotes the drag constant, g is the acceleration of gravity, d^u is the distance from the paddle tail to the center of the UAV, m is the total mass of the individual UAV, I_i denotes the motor rotational inertia, and $|d_i(t)| \le D^u$ denotes the environmental disturbance, where D^u is a bounded positive real number.

The consistent description of the UAV formation requires the participation of its physical quantities such as position, velocity, and acceleration, so its kinematic description should be a second-order system, then the kinematic model of the first UAV can be expressed as:

$$\begin{bmatrix} \dot{x}_i \\ \dot{y}_i \\ \dot{z}_i \\ \dot{v}_{mi} \\ \dot{\varphi}_i \end{bmatrix} = \begin{bmatrix} v_{mi} \cos \varphi_i \\ v_{mi} \sin \varphi_i \\ (z_{ei} - z_i)/\tau_z \\ (v_{emi} - v_{mi})/\tau_m \\ (\varphi_{ei} - \varphi_i)/\tau_\varphi \end{bmatrix} \tag{3}$$

where the vector $L_i = [x_i, y_i, z_i, v_{mi}, v_{zi}, \varphi_i]^T (i = 1, \ldots, n)$ is the state vector of UAVi, v_{mi} is the plane flight speed of UAVi, z_i is the flight altitude of UAVi, a_{zi} is the vertical acceleration of UAVi, $(v_{emi}, z_{ei}, \varphi_{ei})$ is the control command input for plane flight speed, flight altitude, and yaw angle of UAVi, and $(\tau_m, \tau_z, \tau_\varphi)$ is the time constant associated with the flight state.

B. UAV CONSISTENCY ALGORITHM AND GRAPH THEORY

The kinematic model of the UAV cluster can be formulated by the following second-order differential equation:

$$\begin{pmatrix} \dot{C}_i = M_i \\ \dot{M}_i = U_i \end{pmatrix} \quad i = 1, \ldots, n \tag{4}$$

where $C_i \in R^t$ is the state vector of UAVi, $M_i \in R^t$ is the intermediate derivative variable, and $U_i \in R^t$ is the control input of UAVi. Taking the above vector component $c_i, m_i, u_i(c_i \in C_i, m_i \in M_i, u_i \in U_i)$, the consistency algorithm yields:

$$u_i = -\sum_{j=1}^n o_{ij}[\eta_1(c_i - c_j) + \eta_2(m_i - m_j)]i = 1, \ldots, n \tag{5}$$

where $\eta_1 > 0, \eta_2 > 0$, which is the consistency strength adjustment parameter, and o_{ij} is the element from the UAV communication topology adjacency matrix O_n. The following conditions need to be satisfied between UAVs when stable clustering is achieved by the consistency algorithm:

$$\| X_i - X_j \| = E_d(t) \ (i, j = 1, \ldots, n i \ne j)$$
$$\begin{pmatrix} v_{mi} \to v_{mj} \varphi_i \to \varphi_j \\ z_i \to z_j v_{zi} \to v_{zj} \end{pmatrix} \tag{6}$$

where $\|\cdot\|$ is the Euclidean parametrization and $E_d(t)$ is the UAV cluster 3D desired formation function. From the above equation, it can be seen that when the UAV cluster is stable, its relative position converges to the predetermined formation, and the plane velocity, vertical velocity, vertical altitude, and yaw angle converge to values close to each other.

The communication topology of the UAV cluster can be represented by the graph $G_{uav} = \{\boldsymbol{\rho}, \upsilon, O_n\}$, $\boldsymbol{\rho} = \{\rho_1, \ldots, \rho_n\}$ denotes the set of nodes in the topology, $\upsilon = \{(v_i, v_j) \subseteq \boldsymbol{\rho} \times \boldsymbol{\rho}, i \neq j\}$ denotes the set of edges in the topology, and $O_n = [o_{ij}] \in R^{n \times n}$ denotes the adjacency matrix of the topology graph, where $o_{ij} = 1$ if UAV^i and UAV^j can communicate, and $o_{ij} = 0$ otherwise, which can be expressed in the following concrete form:

$$O_n = \begin{pmatrix} & 1 & \cdots & n \\ 1 & o_{11} & \cdots & o_{1n} \\ \vdots & \vdots & \cdots & \vdots \\ n & o_{n1} & \cdots & o_{nn} \end{pmatrix} \quad (7)$$

Defining the degree matrix of a figure G_{uav} as $D_{uav} = \{d(\rho_1), \ldots, d(\rho_n)\}$, where element $d_i = \sum_{j=1}^{n} o_{ij}$, the specific expression of the elements in the Laplace matrix $L_p = D_{uav} - O_n$ of the UAV communication topology is shown in the following equation:

$$l_{uavij} = \begin{cases} o_{ij} & i \neq j \\ \displaystyle\sum_{i \neq j, j=1}^{n} o_{ij} & i = j \end{cases} \quad (8)$$

To ensure that the consistency algorithm achieves convergence, a spanning tree should exist in the communication topology of the UAV, i.e., for any node s in the topology, any node in the topology can be reached from that point.

C. PROBLEM DESCRIPTION

UAVs in cluster formation can compensate for mission execution failures due to the lack of capability of a single UAV. The system model in this paper is shown in Figure 1. Consider n UAVs for cluster reconnaissance, in which there is an enemy strike force in the reconnaissance area, and the enemy will destroy the formation, causing a certain number of UAVs to leave the formation during the cluster mission, which results in topological damage and reconnaissance holes, causing missing reconnaissance data and discontinuous coverage. Therefore, considering enemy strikes, cluster reconstruction is realized by combining consistency theory and sliding mode technology, which effectively solves the problem of UAV cluster topological damage and discontinuous coverage.

The UAVs $1, \ldots, n$ use a 4-connection communication method for square cluster formation to achieve 1 coverage of the reconnaissance area, and the UAVs involved in the cluster do not distinguish the importance of the nodes. Meanwhile, to save resources, no redundant UAVs are configured to act as relays to complete topological reconfiguration and continuous coverage control, and only the remaining UAVs are applied to achieve cluster reconfiguration when the UAV swarm suffers a blow, the schematic diagram of which is shown in Figure 2. Assume that the UAVs in the formation can obtain the coordinates of the UAVs out of the formation $\{(x_{ierr}, y_{ierr}, z_{ierr})i \in ERR\}$, where ERR is the set of UAVs out of the formation, and by the consistency theory, each UAV
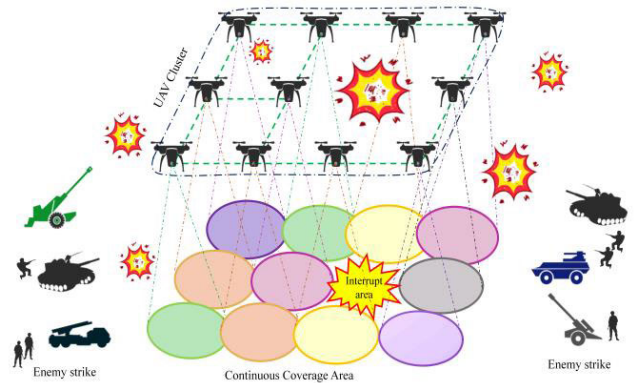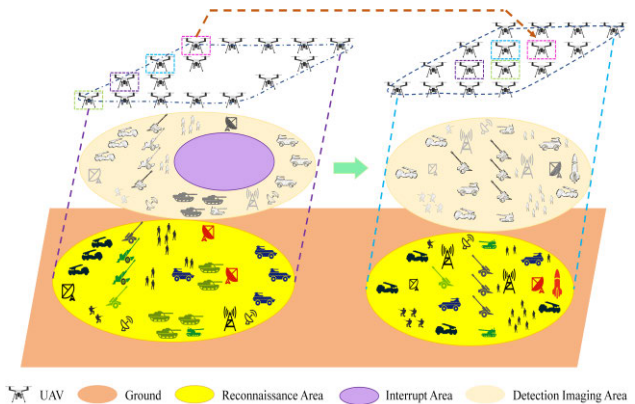

FIGURE 1. System model diagram.

FIGURE 2. Cluster reconfiguration diagram.

will make the formation converge to a stable state through the single-hop neighbor set.

Define the UAV trajectory tracking error $(e_x^{uavl}, e_y^{uavl}, e_z^{uavl})$ and attitude tracking error $(e_\varphi^{uava}, e_\theta^{uava}, e_\psi^{uava})$ as:

$$\begin{cases} e_x^{uavl} = x(t) - xd(t) \\ e_y^{uavl} = y(t) - yd(t) \\ e_z^{uavl} = z(t) - zd(t) \end{cases} \quad \begin{cases} e_\varphi^{uava} = \varphi(t) - \varphi d(t) \\ e_\theta^{uava} = \theta(t) - \theta d(t) \\ e_\psi^{uava} = \psi(t) - \psi d(t) \end{cases} \quad (9)$$

where $(xd(t), yd(t), zd(t))$ is the virtual desired trajectory to be designed and $(\varphi d(t), \theta d(t), \psi d(t))$ is the virtual desired attitude to be designed, and substituting equation (2) into equation (9), the expression for the variation of the UAV dynamics error can be obtained as:

$$\begin{cases} \ddot{e}_x^{uavl} = U_{uav}^{li} R_{U \to G}^{(13)} - \Gamma_{i1}^{uav} \dot{x}_i/m + d_{xi}(t) - \ddot{x}d(t) \\ \ddot{e}_y^{uavl} = U_{uav}^{li} R_{U \to G}^{(12)} - \Gamma_{i2}^{uav} \dot{x}_i/m + d_{yi}(t) - \ddot{y}d(t) \\ \ddot{e}_z^{uavl} = U_{uav}^{li} R_{U \to G}^{(11)} - \Gamma_{i3}^{uav} \dot{x}_i/m - g + d_{zi}(t) - \ddot{z}d(t) \\ \ddot{e}_\varphi^{uava} = U_{uav}^{\varphi i} - d^u \Gamma_{i4}^{uav} \dot{\varphi}_i/I_\varphi + d_{\varphi i}(t) - \ddot{\varphi}d(t) \\ \ddot{e}_\theta^{uava} = U_{uav}^{\theta i} - d^u \Gamma_{i5}^{uav} \dot{\theta}_i/I_\theta + d_{\theta i}(t) - \ddot{\theta}d(t) \\ \ddot{e}_\psi^{uava} = U_{uav}^{\psi i} - d^u \Gamma_{i6}^{uav} \dot{\psi}_i/I_\psi + d_{\psi i}(t) - \ddot{\psi}d(t) \end{cases}$$
$$(10)$$

After the above transformation, the trajectory tracking problem and attitude tracking problem of UAVs are transformed into the error tracking problem.

III. UAV CONTINUOUS COVERAGE CONTROL SCHEME

In this chapter, a UAV continuous coverage control law that integrates consistency theory with sliding mode theory is proposed. Firstly, the UAV cluster formation is realized by the consistency control law, and after the enemy strike, the formation obtains the coordinates out of the formation set, and at the same time starts the detection procedure for repairing the UAV at the end of the formation, to calculate the required movement time and movement direction of this UAV, and design the virtual desired movement trajectory. Finally, the trajectory and attitude tracking is performed by applying the sliding mode theory, which effectively completes the damage repair of the cluster topology and realizes the continuous coverage control of the formation.

A. UAV CLUSTERING BASED ON CONSISTENCY THEORY

Considering the UAV kinematic model in equation (3), the expressions for the control command signals in the three dimensions of plane speed, heading, and altitude are derived as:

$$v_{emi} = v_{mi} + \dot{v}_{mi}\tau_m \quad z_{ei} = z_i + \dot{z}_i\tau_z \quad \varphi_{ei} = \varphi_i + \dot{\varphi}_i\tau_\varphi \quad (11)$$

Considering the desired plane velocity v_{mi}°, flight altitude z_i°, and yaw angle φ_i°, the expression of the UAV cluster control law by the consistency theory is:

$$u_v = -\alpha(v_{mi} - v_{mi}^\circ) - \sum_{j=1}^n o_{ij}(v_{mi} - v_{mj})$$

$$u_z = -\beta(z_i - z_i^\circ) - \sum_{j=1}^n o_{ij}(z_i - z_j)$$

$$u_\varphi = -\sigma(\varphi_i - \varphi_i^\circ) - \sum_{j=1}^n o_{ij}(\varphi_i - \varphi_j) \quad (12)$$

where $\alpha > 0, \beta > 0, \sigma > 0$ is the control gain. Considering the formation situation of the UAV cluster with the control of the UAV cluster to achieve three-dimensional formation, the plane flight velocity v_{mi} is projected orthogonally to the X axis and Y axis directions, i.e., $v_{xi} = v_{mi}\cos\varphi_i$, $v_{yi} = v_{mi}\sin\varphi_i$. Meanwhile, combined with the three-dimensional expected formation function $E_d(t)$ of the UAV cluster, the control law u_{vx}, u_{vy}, u_z can be expressed as:

$$u_{vx} = -\alpha_1(v_{xi} - v_{xi}^\circ) - Lv_x - \alpha_2(Lx - LE_d^x(t))$$

$$u_{vy} = -\gamma_1(v_{yi} - v_{yi}^\circ) - Lv_y - \gamma_2(Ly - LE_d^y(t))$$

$$u_z = -\beta_1(z_i - z_i^\circ) - \beta_2(Lz - LE_d^z(t)) \quad (13)$$

where $\alpha_1, \alpha_2, \beta_1, \beta_2, \gamma_1, \gamma_2 > 0$ is the control coefficient, $E_d^x(t), E_d^y(t), E_d^z(t)$ is the 3D projection component of the UAV formation expectation function, and L is the Laplace matrix corresponding to the 4-connected adjacency matrix, so that the formation transformation of the UAV cluster can be realized by designing different 3D expectation formation functions.
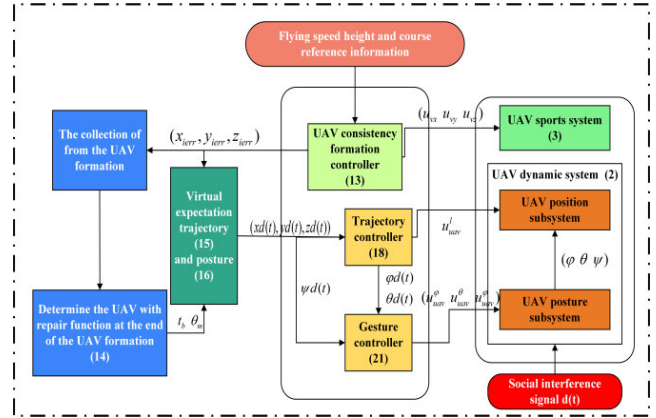

FIGURE 3. UAV cluster continuous coverage control scheme structure diagram.

B. CONTINUOUS COVERAGE CONTROL BASED ON CLUSTER RECONFIGURATION

1) UAV TRAJECTORY TRACKING CONTROL BASED ON NON-SINGULAR FAST TERMINAL SLIDING MODE

The structure diagram of the proposed continuous coverage control scheme based on UAV formation reconfiguration is shown in Figure 3.

When the UAV formation obtains the coordinates in the breakaway formation set, the repair UAV will calculate the time required to move at maximum flight speed t_b with a flight deviation angle of θ_m. where the repair UAV$D^{fb}(uav)$ is determined by:

$$D^{fb}(uav) = \begin{pmatrix} (x_0 + 1, y_0 + 1) \frac{\pi}{4} \leq \varphi \leq \frac{3\pi}{4} \\ (x_{\max} - 1, y_{\max} - 1) - \frac{3\pi}{4} \leq \varphi \leq -\frac{\pi}{4} \\ (X_{\max} - 6, Y_{\max} - 6) \frac{3\pi}{4} \leq \varphi \leq -\frac{3\pi}{4} \\ (X_{\max} = Y_{\max} = ((n - l_y(n)), \ldots, n)) \\ (X_0 + 6, Y_0 + 6) - \frac{\pi}{4} \leq \varphi \leq \frac{\pi}{4} \\ (X_0 = Y_0 = (1, \ldots, l_y(n))) \end{pmatrix}$$

$$(14)$$

where $l_y(\cdot)$ denotes the number of longitudinal UAV units in the formation. Assume that the coordinates of the repair UAV are (x_0^d, y_0^d, z_0^d) then the required movement time t_b and the flight deviation angle θ_m are calculated as:

$$\begin{cases} T_1 = \sqrt{(x_0^d - x_{ierr})^2 + (y_0^d - y_{ierr})^2} \\ \iota_1 = \sqrt{(t_b v_{emi})^2 + (z_{ei} - z_i)^2} \\ \iota_2 = \sqrt{(t_b v_{\max})^2 + (z_{ei} - z_i)^2} \\ T^2 = \dfrac{(T_1)^2 + \iota_1^2 - \iota_2^2}{2\iota_1 T_1} \\ P_1 = \dfrac{\pi}{2} - \arctan(\dfrac{y_{ierr} - y_0^d}{x_{ierr} - x_0^d}) \\ P_2 = \varphi_{ei} \\ \cos(\dfrac{\pi}{2} + P_1 + P_2) = T^2 \\ \theta_m = \arctan(\dfrac{y_{ierr} + t_b v_{emi}\sin(\varphi_{ei}) - y_0^d}{x_{ierr} + t_b v_{emi}\cos(\varphi_{ei}) - x_0^d}) \end{cases} \quad (15)$$

Then the virtual desired motion trajectory $(xd(t), yd(t), zd(t))$ is designed as:

$$\begin{cases} xd(t) = v_{max} \cos(\theta_m) \\ yd(t) = v_{max} \sin(\theta_m) \\ zd(t) = a_b^d t_b^2 + b_b^d t_b + c_b \\ -b_b/2a_b \ge T_1 \\ 4a_b^d c_b - b_b^{d2}/4a_b^d \ge z_{ei} \end{cases} \quad (16)$$

To guarantee that the repair UAV can quickly converge to the desired trajectory, this paper selects a non-singular fast terminal sliding mode method to design the tracking control law, whose sliding surface expression is:

$$H_{x,y,z} = e_{x,y,z}^{uavl} + \frac{1}{\alpha_{x,y,z}^h}(e_{x,y,z}^{uavl})^{d_{x,y,z}^h/b_{x,y,z}^h}$$
$$+ \frac{1}{\beta_{x,y,z}^h}(\dot{e}_{x,y,z}^{uavl})^{p_{x,y,z}^h/q_{x,y,z}^h} \quad (17)$$

where $d_{x,y,z}^h, b_{x,y,z}^h, p_{x,y,z}^h, q_{x,y,z}^h$ is a positive odd number and $1 < p_{x,y,z}^h/q_{x,y,z}^h < 2, d_{x,y,z}^h/b_{x,y,z}^h \ge p_{x,y,z}^h/q_{x,y,z}^h$. The UAV trajectory tracking control law is designed by equations (10), (16), and (17) as:

$$U_{uav}^{li} R_{U \to G}^{(13)} = \Gamma_{i1}^{uav} \dot{x}_i/m + \ddot{x}d(t) - (D^u + \eta_1^u)\text{sgn}(H_x)$$
$$- \frac{\beta_x^h q_x^h}{p_x^h}(\dot{e}_x^{uavl})^{2-\frac{p_x^h}{q_x^h}}(1 + \frac{d_x^h}{\alpha_x^h b_x^h}(e_x^{uavl})^{d_x^h/b_x^h-1})$$

$$U_{uav}^{li} R_{U \to G}^{(12)} = \Gamma_{i2}^{uav} \dot{x}_i/m + \ddot{y}d(t) - (D^u + \eta_2^u)\text{sgn}(H_y)$$
$$- \frac{\beta_y^h q_y^h}{p_y^h}(\dot{e}_y^{uavl})^{2-\frac{p_y^h}{q_y^h}}(1 + \frac{d_x^h}{\alpha_y^h b_y^h}(e_y^{uavl})^{d_y^h/b_y^h-1})$$

$$U_{uav}^{li} R_{U \to G}^{(11)} = \Gamma_{i2}^{uav} \dot{x}_i/m + \ddot{z}d(t) + g - (D^u + \eta_3^u)\text{sgn}(H_z)$$
$$- k^u H_z^{\frac{r^h}{u^h}} - \frac{\beta_z^h q_z^h}{p_z^h}(\dot{e}_z^{uavl})^{2-\frac{p_z^h}{q_z^h}}$$
$$\times (1 + \frac{d_x^h}{\alpha_z^h b_z^h}(e_z^{uavl})^{d_z^h/b_z^h-1})$$
$$(18)$$

where $\eta_1^u > 0, \eta_2^u > 0, \eta_3^u > 0, r^h, u^h$ are positive odd numbers and $r^h/u^h \ge 1$. Due to the under-input characteristics of the UAV, the attitude tracking control is only directly driven for the roll angle to ensure the stability of the reconnaissance. And the yaw angle and pitch angle are tracked and held using the computational expression in (19), as shown at the bottom of the next page, where $[\cdot]^{-1\sim1}$ indicates that values over -1 are taken as -1 and values over 1 are taken as 1.

2) UAV ATTITUDE TRACKING CONTROL BASED ON SLIDING MODE
From the sliding mode theory, the attitude tracking control sliding mode surface is designed as:

$$H_{\varphi,\theta,\psi} = h_{\varphi,\theta,\psi} e_{\varphi,\theta,\psi}^{uava} + \dot{e}_{\varphi,\theta,\psi}^{uava} \quad (20)$$

From equations (10), (19), and (20), the UAV attitude tracking control law is designed as:

$$U_{uav}^{\varphi i} = -h_\varphi \dot{e}_\varphi^{uava} + d^u \Gamma_{i4}^{uav} \dot{\varphi}_i/I_\varphi + \ddot{\varphi}d(t) - k_\varphi^u H_\varphi$$
$$- (D^u + \eta_4^u)\text{sgn}(H_\varphi)$$
$$U_{uav}^{\theta i} = -h_\theta \dot{e}_\theta^{uava} + d^u \Gamma_{i5}^{uav} \dot{\theta}_i/I_\theta + \ddot{\theta}d(t) - k_\theta^u H_\theta$$
$$- (D^u + \eta_5^u)\text{sgn}(H_\theta)$$
$$U_{uav}^{\psi i} = -h_\psi \dot{e}_\psi^{uava} + d^u \Gamma_{i6}^{uav} \dot{\psi}_i/I_\psi + \ddot{\psi}d(t) - k_\psi^u H_\psi$$
$$- (D^u + \eta_6^u)\text{sgn}(H_\psi)$$
$$(21)$$

where, $h_\varphi > 0, h_\theta > 0, h_\psi > 0, k_\varphi^u > 0, k_\theta^u > 0, k_\psi^u > 0, \eta_4^u > 0, \eta_5^u > 0, \eta_6^u > 0$.

3) STABILITY ANALYSIS OF THE CONTROL LAW
To verify the stability of the consistent formation control law, the convergence of the state control equations is now proved, such that $\dot{e}_{v_x} = \dot{v}_{xi} - \dot{v}_{xj}$, then:

$$\dot{e}_{v_x} = -\alpha_1(v_{xi} - \overset{\circ}{v}_x) - \sum_{j=1}^n o_{ij}[(v_{xi} - v_{xj})$$
$$+ \alpha_2(x_i - x_j - x_{id} + x_{jd})]$$
$$+ \alpha_1(v_{xj} - \overset{\circ}{v}_x) + \sum_{k=1}^n o_{jk}[(v_{xj} - v_{xk})$$
$$+ \alpha_2(x_j - x_k - x_{jd} + x_{kd})]$$
$$= -\alpha_1(v_{xi} - v_{xj}) - \sum_{j=1}^n o_{ij}[(v_{xi} - v_{xj}) + \alpha_2(x_i - x_j)]$$
$$+ \sum_{k=1}^n o_{jk}[(v_{xj} - v_{xk}) + \alpha_2(x_j - x_k)]$$
$$= -\alpha_1(v_{xi} - v_{xj}) - Mo_{ij}[(v_{xi} - v_{xj}) + \alpha_2(x_i - x_j)]$$
$$= -(\alpha_1 + Mo_{ij})e_{v_x} - Mo_{ij}\alpha_2 e_x \quad (22)$$

Transforming equation (22) into matrix form expresses:

$$\begin{pmatrix} \dot{e}_x \\ \dot{e}_{v_x} \end{pmatrix} = \begin{pmatrix} 0 & 1 \\ -Mo_{ij}\alpha_2 & -(\alpha_1 + Mo_{ij}) \end{pmatrix} \begin{pmatrix} e_x \\ e_{v_x} \end{pmatrix} \quad (23)$$

In the above equation, $\dot{e}_{v_x}$ denotes the error in the horizontal velocity of the plane between the UAVs. Because $Mo_{ij}\alpha_2 > 0$ and $\alpha_1 + Mo_{ij} > 0$, converge to 0 by the Hurwitz stability criterion $\dot{e}_{v_x}$. Let $e'_{v_x} = v_{xi} - v_x^\circ$, where e'_{v_x} denotes the error between the UAV planar horizontal velocity and the desired velocity, v_{xi} converge to v_x° prove the following:

$$\begin{pmatrix} \dot{e}'_x \\ \dot{e}'_{v_x} \end{pmatrix} = \begin{pmatrix} 0 & 1 \\ 0 & -\alpha_1 \end{pmatrix} \begin{pmatrix} e'_x \\ e'_{v_x} \end{pmatrix}$$
$$+ \begin{pmatrix} 0 \\ \sum_{j=1}^n o_{ij}[(v_{xi} - v_{xj}) + \alpha_2(x_i - x_j - x_{id} + x_{jd})] \end{pmatrix}$$
$$(24)$$

The above equation, $\alpha_1 > 0$, converges to 0 according to the Hurwitz stability criterion e'_{v_x}. The proof for the plane's vertical velocity and height is similar to the plane's horizontal velocity and will not be repeated in this paper.

After the stability of equations (18) and (21) is proved, the effectiveness of trajectory tracking and attitude tracking of UAVs can be guaranteed. For trajectory tracking control, the control method used by (X, Y, Z) three channels is the same, while for attitude tracking control, the control method used by (φ, θ, ψ) is also the same. Therefore, this paper analyzes the stability of UAV height tracking control and roll angle tracking control. For the height tracking control law, define the Lyapunov function V_z with respect to H_z as:

$$V_z = \frac{1}{2}H_z^2 \tag{25}$$

Taking the derivative of V_z and substituting the equation into its derivative expression yields:

$$
\begin{aligned}
\dot{V}_z &= H_z \dot{H}_z \\
&= H_z(\dot{e}_z^{uavl} + \frac{d_z^h}{\alpha_z^h b_z^h}(e_z^{uavl})^{d_z^h/b_z^h-1}\dot{e}_z^{uavl} \\
&\quad + \frac{p_z^h}{\beta_z^h q_z^h}(\dot{e}_z^{uavl})^{p_z^h/q_z^h-1}\ddot{e}_z^{uavl}) \\
&= H_z((1 + \frac{d_z^h}{\alpha_z^h b_z^h}(e_z^{uavl})^{d_z^h/b_z^h-1})\dot{e}_z^{uavl} \\
&\quad + \frac{p_z^h}{\beta_z^h q_z^h}(\dot{e}_z^{uavl})^{p_z^h/q_z^h-1}(U_{uav}^{li}R_{U\to G}^{(11)} - \Gamma_{i3}^{uav}\dot{x}_i/m \\
&\quad - g + d_{zi}(t) - \ddot{z}d(t))) \\
&= H_z((1 + \frac{d_z^h}{\alpha_z^h b_z^h}(e_z^{uavl})^{d_z^h/b_z^h-1})\dot{e}_z^{uavl} \\
&\quad + \frac{p_z^h}{\beta_z^h q_z^h}(\dot{e}_z^{uavl})^{p_z^h/q_z^h-1}(-(D^u + \eta_3^u)\text{sgn}(H_z) + d_{zi}(t) \\
&\quad - k^u H_z^{\frac{r^h}{u^h}} - \frac{\beta_z^h q_z^h}{p_z^h}(\dot{e}_z^{uavl})^{2-\frac{p_z^h}{q_z^h}}(1 + \frac{d_x^h}{\alpha_z^h b_z^h}(e_z^{uavl})^{d_z^h/b_z^h-1}))) \\
&= -H_z(\frac{p_z^h}{\beta_z^h q_z^h}(\dot{e}_z^{uavl})^{p_z^h/q_z^h-1}((D^u + \eta_3^u)\text{sgn}(H_z) - d_{zi}(t)) \\
&\quad - k^u \frac{p_z^h}{\beta_z^h q_z^h}(\dot{e}_z^{uavl})^{p_z^h/q_z^h-1}H_z^{\frac{r^h}{u^h}+1}
\end{aligned}
$$

where $r^h, u^h, p_z^h, q_z^h, k^u$ are positive odd numbers and $r^h/u^h \geq 1, 1 < p_z^h/q_z^h < 2, d_z^h/b_z^h \geq p_z^h/q_z^h$,then:

$$k^u \frac{p_z^h}{\beta_z^h q_z^h}(\dot{e}_z^{uavl})^{p_z^h/q_z^h-1}H_z^{\frac{r^h}{u^h}+1} > 0 \tag{26}$$

From the above equation, it follows that:

$$\dot{V}_z \leq -H_z(\frac{p_z^h}{\beta_z^h q_z^h}(\dot{e}_z^{uavl})^{p_z^h/q_z^h-1}((D^u + \eta_3^u)\text{sgn}(H_z) - d_{zi}(t)) \tag{27}$$

Consider$|d_i(t)| \leq D^u, \eta_3^u > 0$ then equation (27) becomes:

$$\dot{V}_z \leq -\frac{p_z^h \eta_3^u}{\beta_z^h q_z^h}(\dot{e}_z^{uavl})^{p_z^h/q_z^h-1}|H_z| \tag{28}$$

As $p_z^h \eta_3^u(\dot{e}_z^{uavl})^{p_z^h/q_z^h-1}|H_z| \big/ \beta_z^h q_z^h > \varepsilon_+$, at this point $\dot{V}_z < 0$, then H_z, converges to 0 in finite time, the height trajectory tracking control is stable.

For the roll angle attitude tracking control law, define the Lyapunov function V_ψ on H_ψ as:

$$V_\psi = \frac{1}{2}H_\psi^2 \tag{29}$$

Taking the derivative of V_ψ and substituting the equation (10), (14) $\sim$ (15), (20) $\sim$ (21) into its derivative expression gives:

$$
\begin{aligned}
\dot{V}_\psi &= H_\psi \dot{H}_\psi \\
&= H_\psi(h_\psi \dot{e}_\psi^{uava} + \ddot{e}_\psi^{uava}) \\
&= H_\psi(h_\psi \dot{e}_\psi^{uava} + U_{uav}^{\psi i} - d^u\Gamma_{i6}^{uav}\dot{\psi}_i/I_\psi + d_{\psi i}(t) - \ddot{\psi}d(t)) \\
&= H_\psi(-k_\psi^u H_\psi - (D^u + \eta_6^u)sgn(H_\psi) + d_{\psi i}(t)) \tag{30}
\end{aligned}
$$

Considering $k_\psi^u > 0, \eta_6^u > 0$, then $\dot{V}_\psi \leq -k_\psi^u H_\psi^2 - \eta_6^u|H_\psi|$, and since $H_\psi^2 > \varepsilon_+, |H_\psi| > \varepsilon_+$, therefore $\dot{V}_\psi < 0$, then H_ψ converges to 0 in finite time, the roll angle attitude tracking control is stable.

In summary, the consistent formation control law of the UAV and the tracking control law and attitude control law of the repair UAV can both stabilize the control of the UAV and finally achieve topological damage repair and continuous coverage control based on cluster reconfiguration.

IV. SIMULATION ANALYSIS

To verify the effectiveness of UAV formation control based on consistency theory and continuous coverage control based on sliding mode theory. In this paper, two sets of experiments were designed with 36 UAVs in cluster formation. The first set of experiments is to verify the control effect of UAV cluster coverage by applying the control law of equation (13) to UAVs. During the initial formation, the relative positions

$$
\begin{aligned}
U_{uav}^{li'} &= \frac{U_{uav}^{li}R_{U\to G}^{(11)}}{C\psi dC\theta d} \\
\varphi_d &= \arctan(\frac{S(\psi d)C(\psi d)U_{uav}^{li}R_{U\to G}^{(13)} - C^2 U_{uav}^{li}R_{U\to G}^{(12)}}{U_{uav}^{li'}}) \\
\theta_d &= \arcsin(\left[\frac{C(\psi d)(C(\psi d)U_{uav}^{li}R_{U\to G}^{(13)} + S(\psi d)C^2 U_{uav}^{li}R_{U\to G}^{(12)}}{U_{uav}^{li'}}\right]_{-1\sim 1}) \tag{19}
\end{aligned}
$$

TABLE 1. Quadrotor uav system parameters.

Parameters	Value
$m\,/\,(kg)$	2
$g/(m/s^2)$	9.8
$d^u\,/\,(m)$	0.2
$I_\varphi = I_\theta\,/\,(kg \cdot m^2)$	1.25
$I_\psi\,/\,(kg \cdot m^2)$	2.5
$d_{(x-y)i}(t) = d_{(\varphi-\psi)i}(t)\,/\,(m/s^2)$	$0.1\sin(t)$
$\tau_m = \tau_z = \tau_\varphi$	0.1

TABLE 2. Uav control parameters and expectations.

Parameters	Value	Parameters	Value
$\alpha_1 = \alpha_2 = \gamma_1 = \gamma_2$	1	r^h	11
$\beta_1 = \beta_2$	0.05	$k^u_{\varphi,\theta,\psi}$	50
$v^\circ_{xi} = v^\circ_{yi}\,/\,(m/s)$	4	$h_{\varphi,\theta,\psi}$	30
$z^\circ_i\,/\,(m)$	100	$\Gamma^{uav}_{i1} = \Gamma^{uav}_{i2} = \Gamma^{uav}_{i3}$	0.01
$\psi_i\,(rad/s)$	0	$\Gamma^{uav}_{i4} = \Gamma^{uav}_{i5} = \Gamma^{uav}_{i6}$	0.012
$\alpha^h_{x,y,z} = p^h_{x,y,z} = u^h$	5	D^u	0.1
$\beta^h_{x,y,z} = k^u$	1	$\eta^u_1 = \eta^u_2 = \eta^u_3$	0.1
$q^h_{x,y,z} = b^h_{x,y,z}$	3	$\eta^u_4 = \eta^u_5 = \eta^u_5$	0.1
$d^h_{x,y,z}$	7		

of the UAVs should be within their maximum communication radius $r^{uav}_{\max}$ to ensure the 4 connection of the UAV communication topology, where the initial positions of the UAVs and the three-dimensional coordinates of the UAV cluster expectation function $E^{xyz}_d(t)$ are shown in equation (31) at the bottom of the next page. The second set of experiments is to design a virtual desired trajectory for a repair UAV that is out of the formation set to determine the end of the formation, and apply the control laws of equations (18) and (21) to it to drive the repair UAV to reconfigure the formation and verify the continuous coverage control effect of the repair UAV. A comparison between the proposed method and related methods in terms of reconfiguration time is also presented to demonstrate the superiority of the proposed method. The simulation experiments are based on a quadrotor UAV with system model parameters selected as shown in Table 1 [30], [31]:

To prevent the control law from high-frequency oscillations causing system instability, this paper applies the saturation function instead of the symbolic function implementation, where the saturation thickness $\Delta = 0.3$, whose expression is:

$$sign(H)sat^u(H) = \begin{cases} 1 & H > \Delta \\ H/\Delta & |H| \leq \Delta \\ -1 & H < \Delta \end{cases} \quad (32)$$

The UAV formation control parameters and expectations are set with the restoration UAV control parameters and expectations as shown in Table 2 [32].

Considering the UAV spacing distance in equation (31) as 10m, applying equation (13) to the UAV yields the UAV cluster formation trajectory simulation results shown in Figure 4. As can be seen from the detail enlargement, the UAVs eventually converge from their scattered initial positions to the desired formation of the formation, while the direction of the formation movement and the altitude values all achieve the desired effect. At the beginning of the cluster, different height values were preassigned to the 36 UAVs to prevent UAV collisions, and the UAVs achieved the initial construction of the cluster formation in advance through the horizontal control law, during which the distance change curve between each UAV is shown in Figure 5. As shown by the figure, the minimum distance between UAVs is 1.843m, which satisfies the conditions for safe UAV flight. At the same time, due to $\{\alpha_{1,2}, \gamma_{1,2}\} > \beta_{1,2}$, the UAV horizontal control convergence speed will be faster than the height control convergence speed to form the cluster expectation formation in advance, compared with the application of the artificial potential energy method to achieve UAV collision avoidance, the control law proposed in this paper is more concise and faster convergence speed.

From Figure 6, Figure 7 it can be seen that both the X-axis velocity and Y-axis velocity of the UAV cluster formation eventually converge to the expected 4 m/s. From the enlarged detail of Figure 8, it can be seen that the 36 UAV altitude values from the initial different altitudes eventually converge to 100m, satisfying the expected results.

Fig. 9, and Figure 10 show the top view of the trajectory of the UAV cluster horizontal plane axis and axis. As can be seen from its detail enlargement, the position point error of the UAV cluster formation is approximately 0.6% ~ 0.8% relative to the ratio of the desired distance between UAVs, thus showing that the cluster formation effect is accurate and ensures safety and continuity of coverage between UAVs.

Suppose UAV No.26 is detached from the formation after an enemy strike, and the serial number of UAV No.26 appears in the detached formation set with its relative position coordinates. At this point, there is a reconnaissance hole in the UAV cluster coverage, and at the same time, there is damage to the communication topology. At this point, the repair UAV at the end of the formation is detected by equation (14) as UAV No.1, and the desired trajectory of UAV No.1 is obtained through the calculation of equations (15) and (16) as:

$$xd(t) = 4.628t$$
$$yd(t) = 6.526t$$
$$zd(t) = -0.3184t^2 + 5.0473t + 100 \quad (33)$$

The maximum movement speed of the UAV is $v_{\max} = 8$ m/s. To represent the repair trajectory of the repair UAV, the leap height is set to 20m. In the event of multiple cavities, the leap height of each repair UAV is set to be different from each other to ensure the safe operation between repair UAVs. Figure 11 show the simulation results of trajectory tracking and attitude tracking of the repair UAV. The tracking error
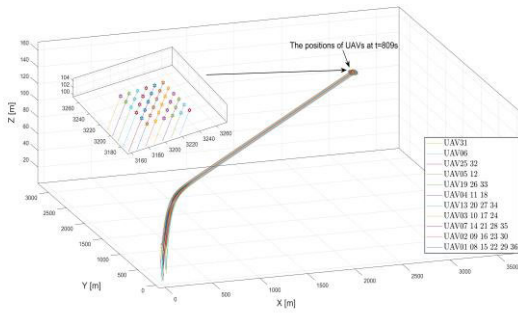
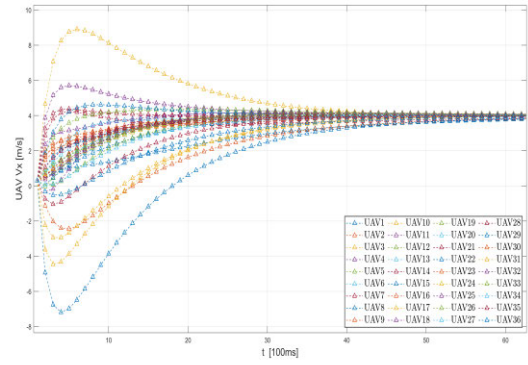**FIGURE 4. UAV formation trajectory diagram.**

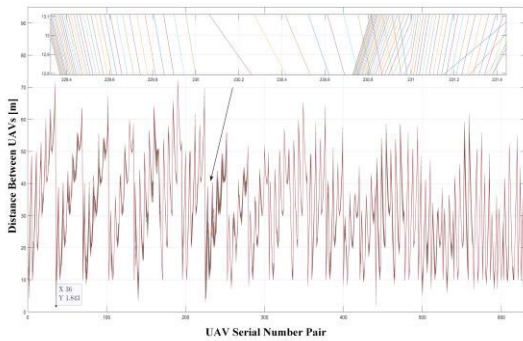**FIGURE 6. Variation curve of X-axis component of each UAV velocity.**

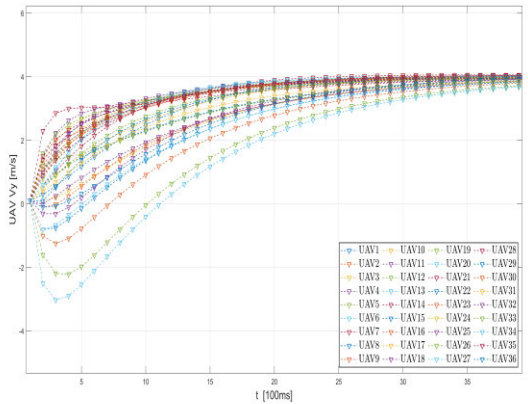**FIGURE 5. Variation of distance between UAVs at the beginning of the cluster.**

FIGURE 7. Variation curve of Y-axis component of each UAV velocity.

e_l^{uav} between X-axis and Y-axis is less than the safe distance between no humans, which can achieve effective cavity filling and topological repair. For the repair process, the attitude of the UAV does not affect its repair effect, so the attitude tracking can be kept stable, and it can also be seen from the figure that each attitude angle tends to be stable. The detailed change of the repair trajectory and formation of the repair UAV can be seen from the detail enlargement in Figure 12.

The UAV cluster reconfiguration problem is transformed into an optimization problem as shown in equation (34). Where **u** denotes the UAV control input, $u_{\min}$, $u_{\max}$ denotes its upper and lower bound constraints, T denotes the cluster

reconfiguration time, h_i denotes the reconfigured formation constraint, g_i is the obstacle constraint between each UAV, l_i is the inter-UAV communication topological distance constraint, and (x_{im}, y_{im}, z_{im}) is the distance between each UAV corresponding to the desired cluster formation.

$$\min_{u,T} J(u, T) = T$$
$$s.t.\ u_{\min} \le u \le u_{\max}, T > 0, \dot{x} = v, \dot{v} = \mathrm{u}$$
$$h_i = \left[x_i(T) - x_m(T) - x_{i,m}\right]^2$$

$$(X, Y, Z)_{initial} = \begin{bmatrix} (6, 1, 34) & (20, 0, 24) & (10, 3, 28) & (2, 30, 10) & (10, 38, 1) & (24, 30, 12) \\ (30, 0, 43) & (40, 7, 36) & (50, 0, 25) & (30, 34, 26) & (40, 30, 15) & (58, 31, 40) \\ (0, 10, 23) & (26, 10, 27) & (20, 15, 21) & (0, 43, 47) & (7, 42, 7) & (20, 44, 44) \\ (30, 10, 42) & (38, 10, 19) & (50, 10, 41) & (40, 40, 5) & (41, 41, 29) & (40, 40, 6) \\ (0, 20, 35) & (8, 20, 4) & (22, 22, 48) & (52, 40, 18) & (50, 40, 8) & (51, 40, 0) \\ (30, 23, 22) & (49, 20, 9) & (45, 23, 33) & (50, 50, 31) & (50, 50, 39) & (55, 53, 32) \end{bmatrix}$$

(31)

$$E_d^{xyz}(t) = \begin{bmatrix} (0, 0, 100) & (10, 0, 100) & (20, 0, 100) & (30, 0, 100) & (40, 0, 100) & (50, 0, 100) \\ (0, 10, 100) & (10, 10, 100) & (20, 10, 100) & (30, 10, 100) & (40, 10, 100) & (50, 10, 100) \\ (0, 20, 100) & (10, 20, 100) & (20, 20, 100) & (30, 20, 100) & (40, 20, 100) & (50, 20, 100) \\ (0, 30, 100) & (10, 30, 100) & (20, 30, 100) & (30, 30, 100) & (40, 30, 100) & (50, 30, 100) \\ (0, 40, 100) & (10, 40, 100) & (20, 40, 100) & (30, 40, 100) & (40, 40, 100) & (50, 40, 100) \\ (0, 50, 100) & (10, 50, 100) & (20, 50, 100) & (30, 50, 100) & (40, 50, 100) & (50, 50, 100) \end{bmatrix}$$
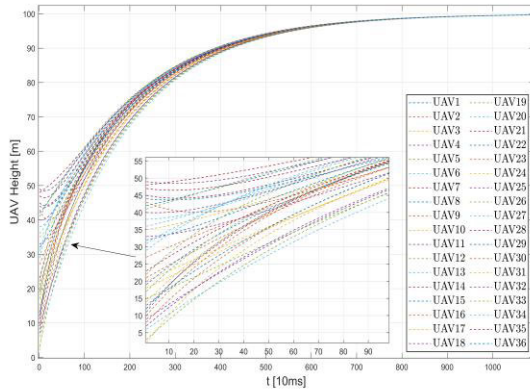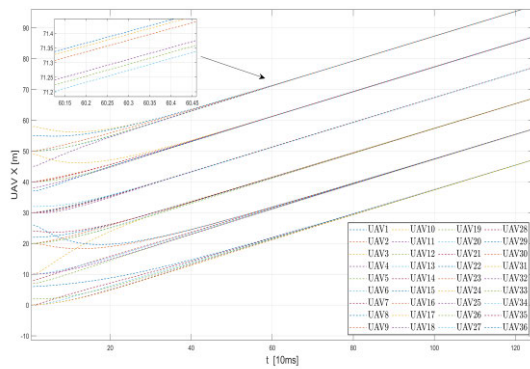
FIGURE 8. Height change curve of each UAV.

FIGURE 9. Variation curve of X-axis component of each UAV position.

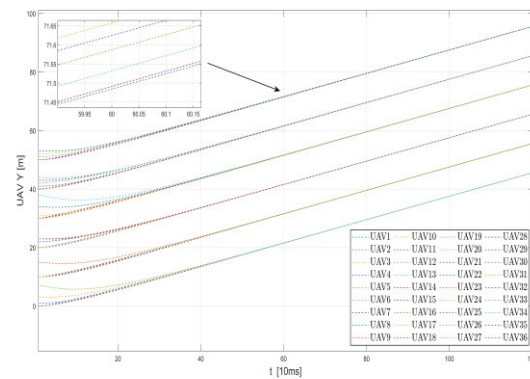**FIGURE 10. Variation curve of Y-axis component of each UAV position.**

$$+ \left[y_i(T) - y_m(T) - y_{i,m} \right]^2$$
$$+ \left[z_i(T) - z_m(T) - z_{i,m} \right]^2 = 0 i, m = 1, 2, \cdots, N$$
$$g_i = d\left(x_i(t), x_j(t) \right) - D_{\text{safe}} \geq 0 \, i$$
$$= 1, 2, \cdots, N(N-1)/2$$
$$l_i = d\left(x_i(t), x_j(t) \right) - D_{\text{comm}} \geq 0 \, i$$
$$= 1, 2, \cdots, N(N-1)/2 \tag{34}$$

For the particle swarm algorithm, the number of particles is 100, the maximum number of iterations is set to 200, the inertia weight is 0.84 and the learning factor is 2.03. For the RRT
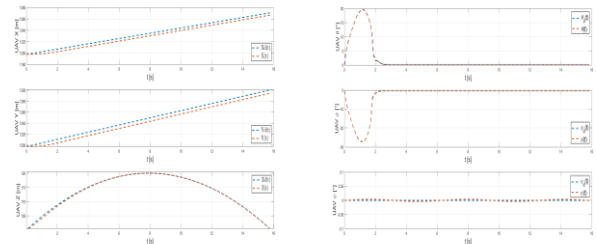

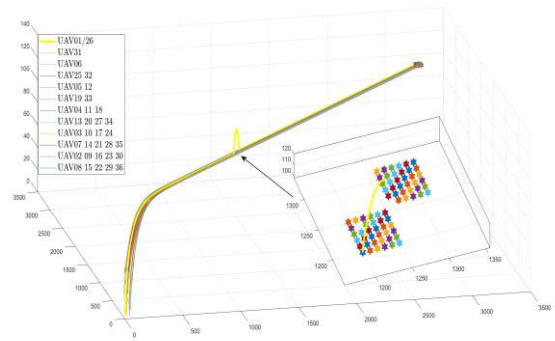**FIGURE 11. Fixing UAV trajectory and attitude tracking maps.**

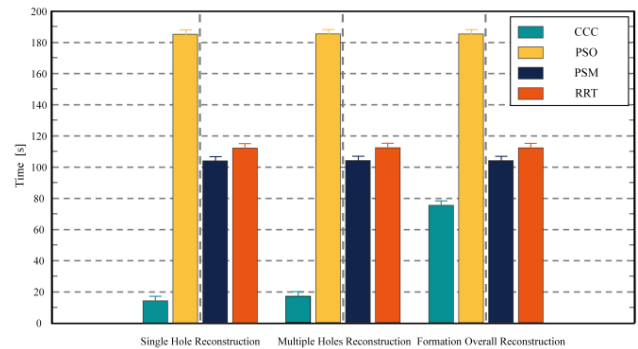**FIGURE 12. UAV cluster reconfiguration with continuous coverage control process diagram.**

FIGURE 13. Plot of UAV cluster reconfiguration time comparison.

algorithm, the sampling probability is set to 0.5, and when reconstruction is needed, the UAV will sample the surrounding environment for the map and completes the formation reconstruction by constant recurrence. The pseudo-spectral method is based on the optimal control toolkit GPOPS for solving the above optimization model.

Fig. 13 shows a comparison of the reconstruction time of the continuous coverage control method (CCC) in this paper with various other algorithms. In the figure, it can be seen that the CCC method proposed in this paper has better time convergence, especially when there are a small number of damage holes in the formation, the algorithm proposed in this paper performs more obviously. In the event of a single reconnaissance hole, only one repair UAV needs to be called to directly replenish the hole, and the formation reconstruction time converges extremely quickly. The convergence time of the formation reconstruction in case

of multiple voids depends on the movement time required to track the repair UAV with the longest path. Under the conditions of the UAV movement parameters set in this paper, the movement time required for the longest path is around 18s, which is much lower than the convergence time of other algorithms. The reason for this is that the other algorithms do not accurately realize the reconfiguration, but instead use a method that drives the whole formation to move, so even if the overall formation movement cost is optimized, the formation reconfiguration convergence time is still too long to meet the requirements of fast reconfiguration in a striking context. In the case of a strike overload, the overall formation needs to be reconfigured, at which point the 3D desired formation function $E_d(t)$ can be updated, at which point the formation convergence time is shown in the third set of data comparisons in the figure.

Simulation results show that the cluster reconfiguration-based CCC method proposed in this paper can achieve the repair of coverage voids and topological damage for UAV cluster formations, effectively improving the destructive resistance and robustness of UAV clusters during missions.

V. CONCLUSION

This paper focuses on a cluster reconfiguration-based UAV CCC method in the context of the crackdown. Firstly, a consistent formation control law is proposed according to the UAV kinematic model, and the process of multiple UAVs from scattering to completing formation is achieved through height pre-distribution. Secondly, the determination method of repairing the UAV when there is a reconnaissance hole and the generation method of virtual expectation trajectory is given to provide an accurate tracking trajectory for realizing formation reconstruction. And then, based on the UAV dynamics model, the trajectory tracking control law and attitude tracking control law of the UAV are proposed by the sliding mode theory to realize the fast-tracking of the UAV in a limited time to repair the hole. Finally, the control law proposed in this paper is analyzed to prove its stability and robustness. The simulation results show that the method proposed in this paper has a good UAV cluster reconfiguration effect, can achieve UAV continuous coverage control quickly and accurately, and guarantee the real-time and anti-destructive performance of UAV cluster formation.

REFERENCES

[1] C. Han, A. Liu, K. An, X. Tong, and X. Liang, "A game-theoretic-based approach for UAV swarm deployment and networking in jamming environment," *J. Electron. Inf.*, vol. 44, no. 3, pp. 860–870, 2022.

[2] S. Li and X. Fang, "A modified adaptive formation of UAV swarm by pigeon flock behavior within local visual field," *Aerosp. Sci. Technol.*, vol. 114, Jul. 2021, Art. no. 106736.

[3] R. Valentino, W.-S. Jung, and Y.-B. Ko, "A design and simulation of the opportunistic computation offloading with learning-based prediction for unmanned aerial vehicle (UAV) clustering networks," *Sensors*, vol. 18, no. 11, p. 3751, Nov. 2018.

[4] X. Gao, L. Wang, X. Yu, X. Su, Y. Ding, C. Lu, H. Peng, and X. Wang, "Conditional probability based multi-objective cooperative task assignment for heterogeneous UAVs," *Eng. Appl. Artif. Intell.*, vol. 123, Aug. 2023, Art. no. 106404.

[5] X. Wang, B. Li, X. Su, H. Peng, L. Wang, C. Lu, and C. Wang, "Autonomous dispatch trajectory planning on flight deck: A search-resampling-optimization framework," *Eng. Appl. Artif. Intell.*, vol. 119, Mar. 2023, Art. no. 105792.

[6] Z. Miao, Y.-H. Liu, Y. Wang, G. Yi, and R. Fierro, "Distributed estimation and control for leader-following formations of nonholonomic mobile robots," *IEEE Trans. Autom. Sci. Eng.*, vol. 15, no. 4, pp. 1946–1954, Oct. 2018.

[7] H. Chen, X. Wang, L. Shen, and Y. Cong, "Formation flight of fixed-wing UAV swarms: A group-based hierarchical approach," *Chin. J. Aeronaut.*, vol. 34, no. 2, pp. 504–515, Feb. 2021.

[8] P. Li, J. Cao, and D. Liang, "UAV-BS formation control method based on loose coupling structure," *IEEE Access*, vol. 10, pp. 88330–88339, 2022.

[9] H. Qiu and H. Duan, "From bird flocking flight to UAV autonomous cluster formation," *J. Eng. Sci.*, vol. 39, no. 3, pp. 317–322, 2017.

[10] J. Zhang, J. Yan, P. Zhang, and B. Wang, "Research on UAV formation obstacle avoidance control based on improved artificial potential field," *J. Xi'an Jiaotong Univ.*, vol. 52, no. 11, pp. 112–119, 2018.

[11] Y. Wu and T. Liang, "UAV formation control based on improved consistency algorithm," *Aeronaut.*, vol. 41, no. 9, pp. 172–190, 2020.

[12] X. Li, L. Wang, H. Wang, L. Tao, and X. Wang, "A warm-started trajectory planner for fixed-wing unmanned aerial vehicle formation," *Appl. Math. Model.*, vol. 122, pp. 200–219, Oct. 2023.

[13] Y. Wu, J. Gou, X. Hu, and Y. Huang, "A new consensus theory-based method for formation control and obstacle avoidance of UAVs," *Aerosp. Sci. Technol.*, vol. 107, Dec. 2020, Art. no. 106332.

[14] J. Gou, T. Liang, and C. Tao, "UAV formation control and assembly method based on consistency theory," *J. Beijing Univ. Aeronaut. Astronaut.*, pp. 1–12, 2023.

[15] H. Qiu and H. Duan, "A multi-objective pigeon-inspired optimization approach to UAV distributed flocking among obstacles," *Inf. Sci.*, vol. 509, pp. 515–529, Jan. 2020.

[16] C. Tao, R. Zhang, Z. Song, B. Wang, and Y. Jin, "Multi-UAV formation control in complex conditions based on improved consistency algorithm," *Drones*, vol. 7, no. 3, p. 185, Mar. 2023.

[17] Z. Yan, L. Han, X. Li, X. Dong, Q. Li, and Z. Ren, "Event-triggered formation control for time-delayed discrete-time multi-agent system applied to multi-UAV formation flying," *J. Franklin Inst.*, vol. 360, no. 5, pp. 3677–3699, Mar. 2023.

[18] J. Hartley, H. P. H. Shum, E. S. L. Ho, H. Wang, and S. Ramamoorthy, "Formation control for UAVs using a flux guided approach," *Expert Syst. Appl.*, vol. 205, Nov. 2022, Art. no. 117665.

[19] M. S. Ghahroudi, A. Shahrabi, and T. Boutaleb, "A distributed self-organising node deployment algorithm for mobile sensor networks," *Int. J. Commun. Syst.*, vol. 35, no. 16, Nov. 2022, Art. no. e5309.

[20] C. Yang, S. Su, X. Ju, and J. Song, "A mobile sensors dispatch scheme based on improved SOM algorithm for coverage hole healing," *IEEE Sensors J.*, vol. 21, no. 18, pp. 21080–21089, Sep. 2021.

[21] D. Morilla-Cabello, L. Bartolomei, L. Teixeira, E. Montijano, and M. Chli, "Sweep-your-map: Efficient coverage planning for aerial teams in large-scale environments," *IEEE Robot. Autom. Lett.*, vol. 7, no. 4, pp. 10810–10817, Oct. 2022.

[22] W. Gu, J. Tang, L. Bai, and S. Lao, "Optimal efficiency model for time-coordinated multi-UAV formation transformation," *J. Aeronaut.*, vol. 40, no. 6, pp. 192–200, 2019.

[23] Q. Mao, X. Li, and Z. Wang, "Rule-based UAV formation construction and reconfiguration control method," *Syst. Eng. Electron. Technol.*, vol. 41, no. 5, pp. 1118–1126, 2019.

[24] S. Ma, C. Dong, M. Ma, and Q. Wang, "Adaptive communication topology-based quadrotor UAV formation reconfiguration control," *J. Beijing Univ. Aeronaut. Astronaut.*, vol. 44, no. 4, pp. 841–850, 2018.

[25] Y. Li, W. Han, Q. Chen, and Y. Zhang, "Research on multi-UAV formation reconfiguration method based on fast extended random tree algorithm," *J. Northwestern Polytech. Univ.*, vol. 37, no. 3, pp. 601–611, 2019.

[26] Y. Wang, Y. Yue, M. Shan, L. He, and D. Wang, "Formation reconstruction and trajectory replanning for multi-UAV patrol," *IEEE/ASME Trans. Mechatronics*, vol. 26, no. 2, pp. 719–729, Apr. 2021.

[27] C. Gao, J. Ma, T. Li, and Y. Shen, "Hybrid swarm intelligent algorithm for multi-UAV formation reconfiguration," *Complex Intell. Syst.*, vol. 9, no. 2, pp. 1929–1962, Apr. 2023.

[28] S. Zhou, Y. Kang, X. Shi, S. Dai, and C. Zhou, "An autonomous reconfiguration control method for multi-UAV formations based on RQPSO-DMPC," *J. Beijing Univ. Aeronaut. Astronaut.*, vol. 43, no. 10, pp. 1960–1971, 2017.

[29] X. Yang, H. Deng, Y. Gui, and D. Li, "Parameter estimation-based adaptive robust path-following controller for quadrotor UAV," *Soldier Eng.*, vol. 43, no. 8, pp. 1926–1938, 2022.

[30] J. Liu, *Sliding Mode Variable Structure Control MATLAB Simulation*. Beijing, China: Tsinghua University Press, 2005.

[31] D. Yan, W. Zhang, H. Chen, and J. Shi, "Study on multi-UAV sliding mode consistent formation control with time delay and interference constraints," *J. Northwestern Polytech. Univ.*, vol. 38, no. 2, pp. 420–426, 2020.

[32] Z. Zhao, L. Xiao, B. Jiang, and D. Cao, "Fast non-singular terminal sliding mode trajectory tracking control for quadrotor UAV based on dilated state observer," *Control Decis.*, vol. 37, no. 9, pp. 2201–2210, 2022.

GUIFEN CHEN received the B.S. and M.S. degrees in information and communication engineering from Jilin University, China, in 1986 and 1991, respectively, and the Ph.D. degree in optical engineering from the Changchun University of Science and Technology, China, in 2009. She is currently a Professor in information and communication engineering with the Changchun University of Science and Technology. Her research interests include optical information and wireless communication technology, the Internet of Things, and sensor networks.

ZICHEN SUN received the bachelor's degree from the Changchun University of Science and Technology, in 2017, where he is currently pursuing the master's degree. His research interests include self-organized communication resource optimization and UAV communication topology control and reconfiguration.

XINGLONG GU received the bachelor's degree from Changchun University, in 2016. He is currently pursuing the Ph.D. degree with the Changchun University of Science and Technology. His research interests include self-organizing network communication, UAV cluster formation, mission planning, and communication resource optimization.

YIMING SUN received the bachelor's degree from Changchun University, in 2018. He is currently pursuing the master's degree with the Changchun University of Science and Technology. His research interests include self-organized network access and UAV cluster algorithm design and optimization.

• • •